Algerian Bentonite Bridged for removes cationic dye from aqueous solutions by adsorption: Modelling, optimization and kinetics study

Fatima Zohra Batana[1,#]; Mohamed Nadjib Rebizi[2,*]; Abdenacer Guibadj[1]
[1]Physical Chemistry of Materials Laboratory, University of Amar Telidji, Laghouat, Algeria
[2]Organic Chemistry and Natural Substances Laboratory, University of Zian Achour, Djelfa, Algeria
*rebizi-nadjib@hotmail.fr #fzbatana@gmail.com

Abstract

This work includes studying the removal of methylthionine chloride on bridged bentonite, and conducting a batch system adsorption test. The influence of various parameters like the dose of adsorbent, pH, contact time and temperature on the behavior of the MC was studied. The pseudo second order kinetic model seems adequate and correlates with the experimental results. The adsorption isotherm fitted well to the Langmuir model with a maximum adsorption capacity adequate to 45.68 mg g^{-1}. The values of the thermodynamic parameters (ΔH°, ΔG°, and ΔS°) are negative indicating that the method of MC removal by the bentonite is exothermic, spontaneous, and with increasing order at the solid-solution interface. The results of the FTIR, XRD, SEM and BET characterizations show that this bentonite may be a mixture of Montmorillonite, Kaolinite, Illite, Quartz and Calcite, with a specific surface estimated at 30,3961 m^2 g^{-1}.

Keywords: Bentonite, Methylthionine chloride, Adsorption, Kinetics, Thermodynamics, Isotherm

1. Introduction

Since ancient times man has tried to include dyes in many sectors including paper, textile, cosmetics, leather and food industries, 15 to 20% of dyes in these processes are discharged with liquid effluents to the receiving environment often without any prior treatment (Azbar et al., 2004). These products discharged and transported by wastewater are toxic and cause many problems on the environment and human and animal health, for their physicochemical characteristics such as low biodegradability, persistent colour, high concentration of oxidizable substances, high pH and temperature (Arenas et al., 2017).

The industry's choice of synthetic dyes is usually based on the ease of synthesis and photo-catalytic stability. Among them, methylthionine chloride may be a cationic dye, most ordinarily used for dyeing cotton, wood and silk. From an environmental point of view, it becomes vital to eliminate the colored compounds from the effluents (Ahmed et al., 2017).

A variety of treatment processes are often wont to remove coloured pollutants in wastewater, such as coagulation-flocculation, adsorption, photodegradation, biodegradation, chemical oxidation, precipitation, ion exchange (Ahmad et al., 2015; Azizian et al., 2009).

Among the above methods, adsorption is taken into account to be the foremost effective and beneficial method for removing dye due to its convenience and ease. This system has become an analytical method of choice, which is extremely effective in its use (Annadurai et al., 2002).

Activated carbon has become the foremost widely used adsorbent due to its high adsorption capacity (Kannan & Sundaram, 2001) however, due to its high cost, natural adsorbents that are cheap, renewable,

resource-rich and inexpensive, such as agricultura (Kaur et al., 2013) or organic wastes, natural biopolymers (Vakili et al., 2014) and natural clay (Kara et al., 2003) is essential. Many studies have focused on the event of adsorbents from various wastes such as chitin and chitosan (Elwakeel et al., 2021), sugar beet pulp (Tahir et al., 2017), tea waste (Panneerselvam et al., 2011) and clay (Ordonez et al., 2020).

We studied the removal of methylthionine chloride by adsorption on local bentonite, a type of clay found abundantly within the Maghnia region of Algeria. The latter has been organo-modified so as to review its efficiency within the removal of the dye.

Before its use, this bentonite was characterized by Fourier Transform Infrared Spectroscopy (FTIR), X-ray Diffraction (XRD), Scanning Electron Microscope (SEM) and Brunauer-Emmett-Teller (BET).

It is interesting to know how the methylthionine chloride interacts with the surface of the adsorbent, hence the importance of studying the kinetics of adsorption, thermodynamics and the mechanism of adsorption, as well as the optimization of operational conditions for the adsorption process.

2. Materials and methods

2.1 Methylthionine chloride

Methylthionine chloride MC is used as an adsorbent without any purification. Its formula is $C_{16}H_{18}N_3SCl$ (Figure 1) and its molar mass is 319.85 mol g^{-1}. A stock solution of 1000 mg. l^{-1} was prepared by dissolving a weighed amount of methylthionine chloride in 100 mL of distilled water. The test solution (10 mg l^{-1}) was prepared by diluting the stock solution with distilled water.

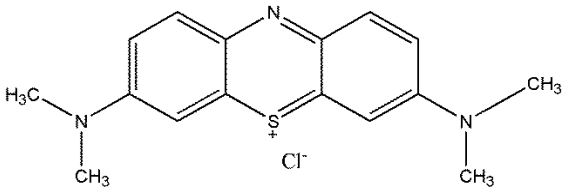

Figure 1: Methylthionine chloride [3,7-bis (dimethylamino) phenazathionium chloride].

Acrylic acid (Sigma-Aldrich 99%) is an analytical grade reagent and can be used without further purification.

2.2 Preparation and characterization of the adsorbent

The bentonite utilized in this study was obtained from the local company ENOF, located in the fields of Mostaganem in Algeria.

2.2.1 Purification and sodification of the raw bentonite

Before use, the raw bentonite was sodiumized 5 times with (NaCl, 1M) for 8 hours, then washed continuously with distilled water to get rid of salt. The obtained bentonite was dried at 80°C, then crushed and sieved.

2.2.2 Bridging of sodium bentonite

The acrylic acid bridged bentonite noted B-Acr was obtained by the dispersion of 3g of sodium bentonite in a solution of acrylic acid $CH_2CHCOOH$ (0.02M) in the presence of 0.2 g of Potassium Persulfate $K_2O_8S_2$. The mixture was stirred at a speed equal to 300 rpm for 10 hours. The resulting product was dried for 24 hours at 60°C and ground.

2.2.3 Characterisation of the adsorbent

B-Acr was characterized using Fourier transform infrared (Jasco 4600 FTIR) as pressed KBr pellets (5% sample and 95% KBr) during a frequency range of 400 cm^{-1}

to 4000 cm^{-1}. The X-ray diffraction (XRD) powder pattern of B-Acr was recorded on a X'Pert PRO PANalytical diffractometer was performed with radiation (Cu K_α = 1.54060 Å). Diffractograms were performed in the 2θ range between 15° and 70°. Scanning electron microscope analysis of the TESCAN Easy Probe type (of high resolution) was performed to obtain images on straight sections of the studied samples. The Brunauer-Emmett-Teller (BET) area and therefore the porous property of B-Acr were measured by determining the N_2 adsorption isotherm at -196°C with an adsorption analyser (Micromeritics ASAP 2020 Plus 2.00). Before adsorption, the sample was degassed under vacuum at 120°C for 12 hours.

2.3 Adsorption tests

All adsorption experiments were performed in batch mode using an Ovan shaker (stirring speed 250 rpm) with temperature control (Basic Magmix MBG05E). Use bridged bentonite to adsorb MC from the aqueous solution in a closed vial containing 100 mL of the solution. The entire experimental campaign was conducted at 298 ± 1 K in order to evaluate the effect of pH, adsorbent dose (m, in g), and contact time (t, in min) on methylthionine chloride removal. Similarly, the influence of temperature (T, in K) was also evaluated. All samples were centrifuged (Sinal TD4 A) to remove any suspended B-Acr particles and the supernatant liquid was analysed by SP-3000 U.V-Visible (nano OPTIMA) to determine the residual dye concentration at a given time (C_e, in mg. L^{-1}). The adsorption capacity (q, in mg. g^{-1}) and the percent removal of MC (R%) were obtained using equations (1) and (2),

$$q_e = (C_0 - C_e)\frac{V}{m} \qquad (1)$$

Where C_0 is the initial concentration of adsorbate in the solution (mg. L^{-1}) and V (l) is the experimental volume of the aqueous solution.

$$R(\%) = 1 - \left(\frac{C_e}{C_0}\right).100 \qquad (2)$$

Three kinetic models, pseudo-first-order, pseudo-second-order and intra-particle diffusion models, are studied to review the kinetic data of methylthionine chloride removal. The pseudo-first-order linear equation is given by the equation (3)

$$Ln(q_e - q_t) = -k_1 t + Ln\ q_e \qquad (3)$$

Where k_1 (min^{-1}) is rate constant for the first-order model. The pseudo-second-order kinetic model is considered to be the most suitable to describe the kinetic adsorption experiment. The linear form equation of this model is given by equation (4)

$$\frac{t}{q_t} = \frac{1}{q_t}t + \frac{1}{k_2 \cdot q_e^2} \qquad (4)$$

Where k_2 (g. $mg^{-1}.min^{-1}$) is the rate constant of the second-order model.

Process the data to check the role of diffusion in the adsorption process. The intraparticle diffusion rate parameter of the dye is determined using the following equation.

$$q_t = K_{id}.t^{0,5} + C \qquad (5)$$

Where K_{id} is intraparticle diffusion rate (mg. g^{-1}. $min^{0.5}$).

The experimental data of equilibrium adsorption isotherms for MC into B-Acr were modelled using the most frequently used isotherms, Langmuir, Freundlich and Temkin.

The Langmuir model is the most widely used isotherm equation, which has the following form:

$$q_e = \frac{q_m K_L C_e}{1 + K_L C_e} \quad (6)$$

Where q_m and K_L are Langmuir isotherm parameters representing the maximum uptake capacity per unit of bentonite mass (mg. g^{-1}) and the Langmuir constant (L. mg^{-1}), respectively.

To predict the adsorption efficiency of the process, the dimensionless equilibrium parameter (R) is expressed by equation (7)

$$R_L = \frac{1}{(1 + K_L . C_0)} \quad (7)$$

The adsorption process is unfavourable when R > 1, favourable when 0 < R < 1, linear when R = 1 and irreversible when R = 0.

The Freundlich isotherm equation has the subsequent form:

$$q_e = K_F C_e^{\frac{1}{n}} \quad (8)$$

where k_F is the Freundlich constant associated with the adsorption capacity $(mg/g)(mg/L)^n$ and parameter n characterizes the heterogeneity of the system.

The Temkin isotherm equation has the following form:

$$q_e = \frac{RT}{b} \mathrm{Ln}\ (A.C_e) \quad (9)$$

3. Results and discussion

3.1 Fourier transform infrared spectroscopy FTIR

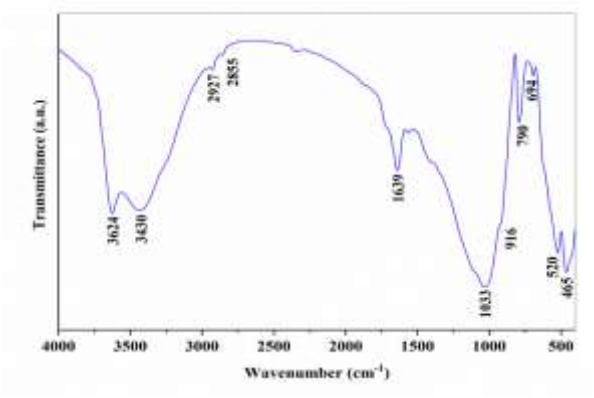

Figure 2: Infrared spectrum of bentonite-acrylic.

Characteristic vibration peaks of hydroxyl groups, silicates and cations are mentioned in the following table 1.

Table 1: Main characteristic IR bands of the studied bentonite.

Bands (cm^{-1})	Interpretations
3624	Octahedra stretching with OH Corners linked to Al or Mg
3430	Absorbed water stretching
2927	Stretching vibration of the C-H bonds of the aliphatic chain
2855	
1639	Absorbed water bending
1033	In plane Si-(Al)-O stretching
916	Al-OH-Al bending
790	Mg-OH-Fe bending
694	Si-O-Si quartz
520	Si-O-Al bending in tetrahedra
465	Si-O-Mg bending in tetrahedra

Generally, two absorption bands that appear at (2927 cm^{-1} and 2855 cm^{-1}) Corresponding to the structure of bentonite and kaolinite O-H hydroxyl elongation vibration (Vicente-Rodríguez et al., 1996). We note the presence of characteristic bands at (2927 cm^{-1} and 2855 cm^{-1}) for the elongation vibration of the C-H bonds of the aliphatic chain (Batana et al., 2019; Marsal et al., 2009) this indicates that the organic group is present with the bentonite. Another average band extends between 1600 cm^{-1} and 1700 cm^{-1}, this band is

centred around 1639 cm^{-1}, is attributed to the deformation vibrations of the O-H bond of the water of constitution and to the deformation vibrations of the bonds of the water molecules adsorbed between the sheets (Yang et al., 2018). An intense absorption band between 900-1200 cm^{-1}, this band is centred around 1033 cm^{-1}, it characterizes the valence vibrations of the Si-O bond (Hameed, 2007; Lv et al., 2007). The angular vibration of the Al-OH group appears as a low-intensity band near 916 cm^{-1} (Nabbou et al., 2019; Yang et al., 2018). The bands between 530 cm^{-1} and 516 cm^{-1} are attributed to the deformation of Si-O-Al^{VI} (VI corresponds to the octahedral position). The bands between 475 cm^{-1} and 450 cm^{-1} are characteristic of the deformation of Si-O-Mg^{VI} that is confirmed by the presence of montmorillonite (Ting et al., 2021). These results are in agreement with those found from DRX (Batana et al., 2019). They confirm the presence of Quartz, Kaolinite, Montmorillonite and Illite in the studied bentonites according to figure 2.

3.1.1 Ray Diffraction XRD

In some favourable cases, the associated minerals in the bentonite are often identified by their main peaks.

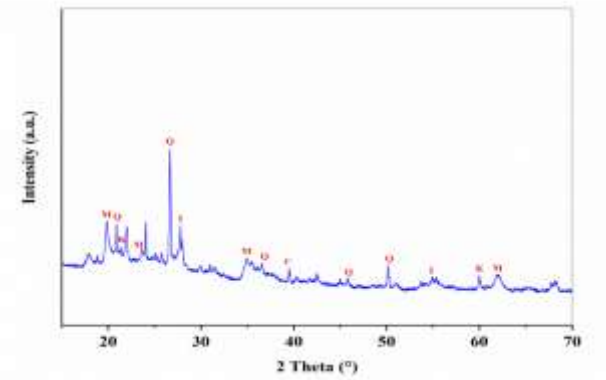

Figure 3. Diffractogram of bentonite-Acr. (K = Kaolinite, I = Illite, Q = Quartz, C= Calcite, M= Montmorillonite).

Therefore, as shown in the diffractogram presented in Figure 3 on B-Acr can easily be identified: Lines at 2θ = 19.72°, 23.54°, 34.72° and 62.03° characteristic of Montmorillonite (M); Lines at 2θ = 20.8°, 26.6°, 36.6°, 45.8° and 50.1° characteristic of Quartz (Q); Lines at 2θ =21.9° and 59.9° characteristic of Kaolinite (K); Lines at 2θ = 27.7° and 54.8° characteristic of Illite (I) (Er-ramly & Ider, 2014). Preliminary examination of the bentonite diffractogram highlights the predominance of silica (SiO_2) in the quartz crystal form indicated by an intense peak. The diffractogram also reveals the presence of Montmorillonite ($(Al_{1.67}Mg_{0.33})Si_4O_{10}(OH)_2Na_{0.33}$),Kaolinite ($Al_2Si_2O_5(OH)_4$), Illite (K, H_3O) and Calcite ($CaCO_3$) (Batana et al., 2019).

3.2 Scanning electron microscopy SEM

According to the SEM observation of the acrylic bridged bentonite sample, the image reported in Figure 4 shows that the surface is covered by well-separated small particles (Praus et al., 2006).

It can also be observed that the surface morphology of the B-Acr particles consists of assemblies of parallel clay sheets forming a compact structure (Makar & Chan, 2008; Sarier et al., 2010).

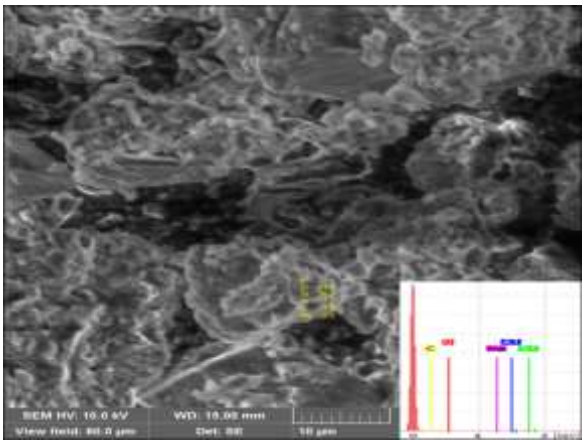

Figure 4: Scanning electron microscope observation of bentonite-Acr.

The surface of the adsorbent appears to be irregular and porous. Supported this, it is often concluded that the adsorbent has an adequate morphological level for the adsorption of the studied pollutant (Benfarhi et al., 2005).
EDX analysis shows that oxygen (44.2%) and silicon (36.5%) are the main components of bentonite. In addition, Al (12.7%), C (3.9%) and Mg (2.6%) (Chebbi et al., 2021).

3.3 BET

N_2 adsorption by B-Acr (Figure 5) follows type IV according to the BET classification (Yuan et al., 2012), it shows the existence of multilayer adsorption and mesopores. The hysteresis loop is of type H_3. The latter is obtained for particles with parallel plate shaped pores (Naranjo et al., 2015).

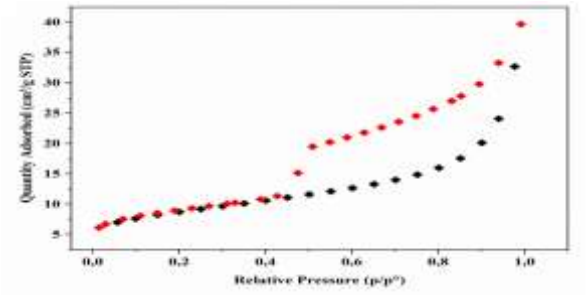

Figure 5: N_2 adsorption–desorption isotherms of bentonite-Acr.

The specific surface calculated by BET transform is estimated to be 30.396 $m^2.g^{-1}$. This specific surface area is considered to be low in comparison with usual adsorbents (Bessaha et al., 2019). The average pore diameter and pore volume are 11.465 nm and 0.055779 cm^3/g respectively (Ghosh et al., 2004). The average particle size is 197.394 nm.

3.4 Effect of adsorbent quantity

The effect of the amount of bentonite and the time of contact on the amount adsorbed and the percentage removal of methylthionine chloride are shown in figures 6 and 7 respectively.

Figure 6 show that the amount of dye adsorbed decreases with the addition of adsorbent

It can be seen that the curves are somewhat identical, i.e., a very fast adsorption is noticed, and then a saturation plateau is reached after 15 to 30 minutes for masses ranging from 0.010 g to 0.020 g.

This behaviour can be explained by:

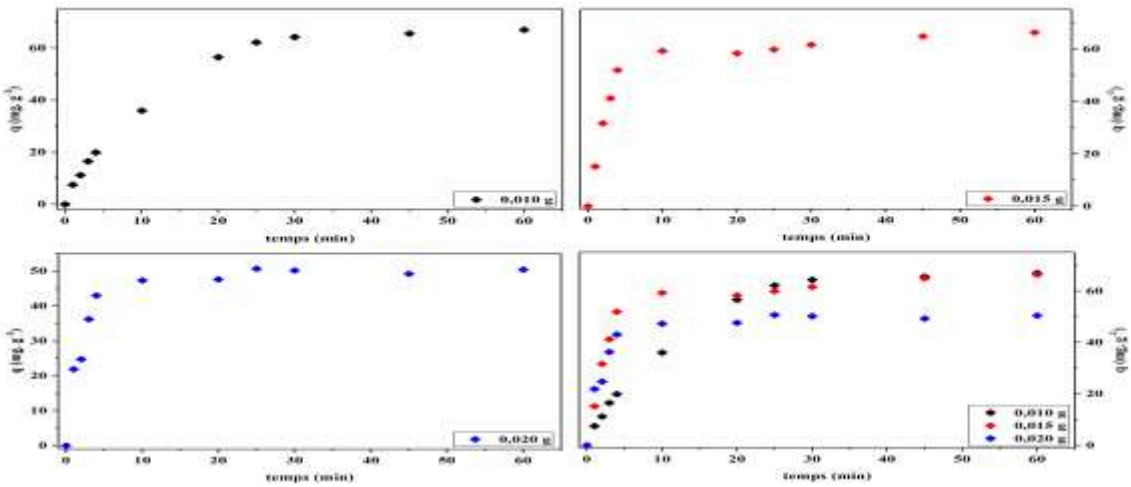

Figure 6: Effect of adsorbent amount on MC adsorption (C_0 = 10 mg. L^{-1}, v=250 rpm).

On the one hand, as long as the amount of adsorbent added to the dye solution is small, the dye cations can easily access the adsorption sites. The addition of bentonite increases the number of adsorption sites but the cations of the dye have more difficulties to approach these sites because of the bulk; and on the other hand, a large amount of bentonite creates particle agglomerations, resulting in a reduction of the total adsorption surface and, consequently, a decrease in the amount of methylthionine chloride fixed per unit mass of adsorbent (Yu et al., 2000) and the non-saturation of the adsorption sites (Karim et al., 2010). For the rest of the experiments, we used a mass of 0.015g of bridged bentonite.

In order to obtain more results, we plotted the removal efficiency R (%) versus time for different bentonite masses (Figure 7).

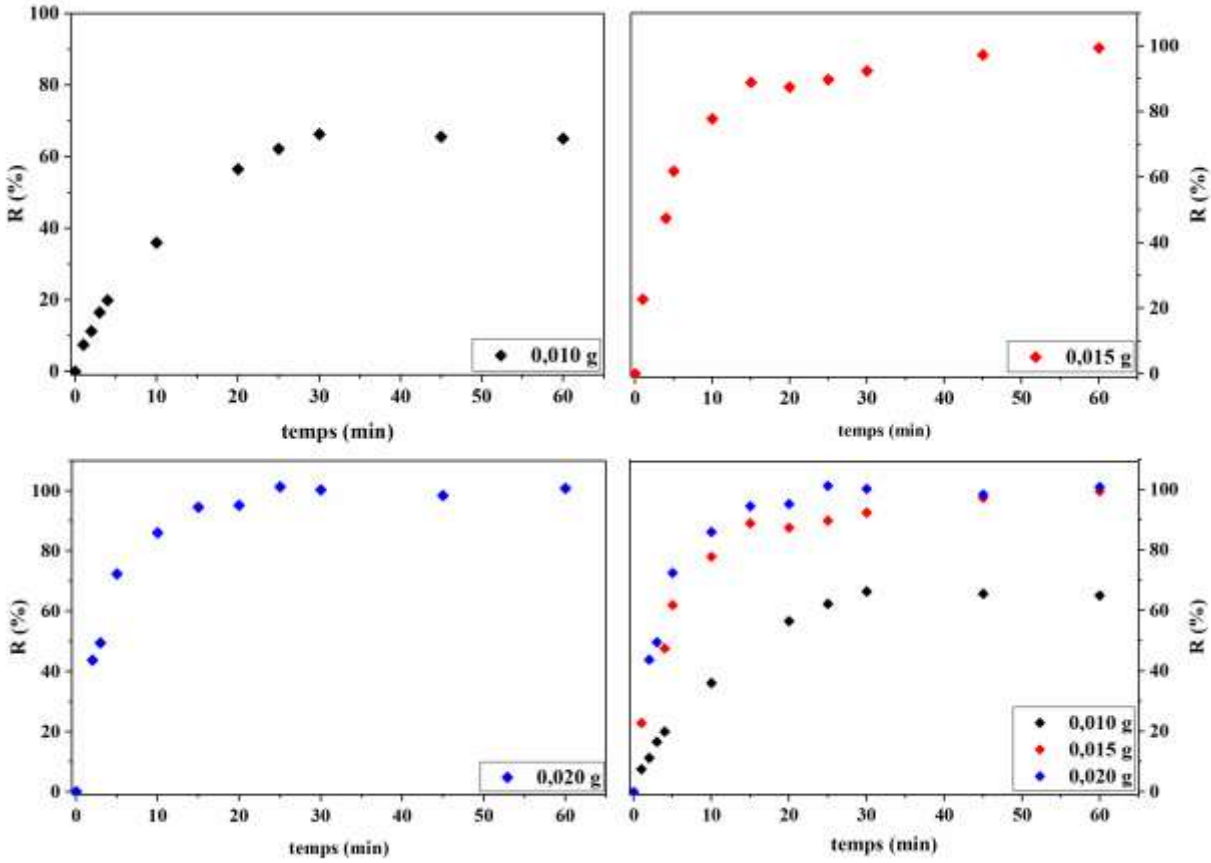

Figure 7: Effect of adsorbent mass on MC adsorption yield (C_0= 10 mg. L^{-1}, v= 250 rpm).

From Figure 7, when the increase in the quantity of the adsorbent means that the surface area of the bentonite is larger, and therefore the number of possible active sites is greater.

The maximum efficiency is obtained by bridged bentonite which is 66.27% for a mass of 0.010 g of bentonite, while it is 99.43% and 100% for a mass of 0.015 g and 0.020 g respectively.

3.5 Effect of pH on adsorption

We studied the evolution of the adsorbed amount of the cationic dye for different pH values (2 to 10), the latter is adjusted by

adding acid HCl (0.1M) or caustic soda NaOH (0.1M). The results shown in Figure 8.

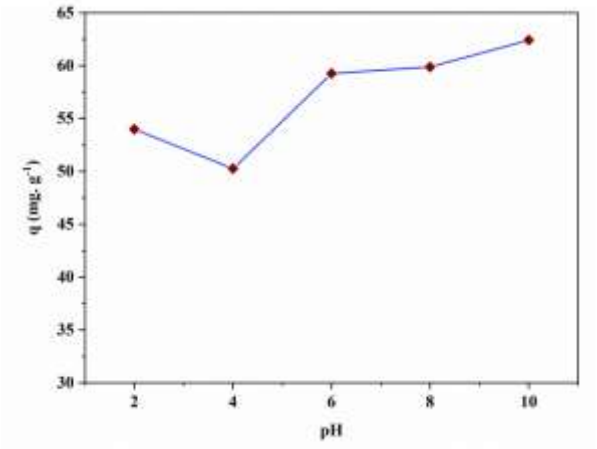

Figure 8: Effect of solution pH on MC adsorption on bridged bentonite (C_0 =10 mg. L^{-1}, v = 250 rpm, t = 30 min).

Figure 8 shows that the basic medium is rather favourable for the adsorption of MC on the studied material than the acidic medium, this may be due to the fact that the addition of H^+ protons lead neutralize the negative charge of bentonite (Patil & Shrivastava., 2010).

The low removal rate of MC in acidic medium can be justified by the fact that the adsorbent's surface is surrounded by H^+ ions which decreases the contact between the MC (cationic pollutant) and the sites of the adsorbent due to electrostatic repulsion and competition between H^+ ions and the cationic dye for adsorption sites (Pérez-Marín et al., 2007). The good interaction in basic medium and which results in a rise of the adsorbed quantity which reaches the worth of 62.41 mg. g^{-1} at pH = 10 would flow from to the very fact that the surface of the bentonite is negatively charged resulting in a robust attraction with the positively charged MC (Sakr et al., 2015). For the rest of the experiments, the pollutant solutions will be taken at their initial pH.

3.6 Effect of temperature on adsorptionion

Temperature has a major effect on the adsorption process of methylthionine chloride using bentonite which was studied for a temperature range between 293 K and 318 K.

Figure 9 shows the influence of temperature on the amount of dye retained.

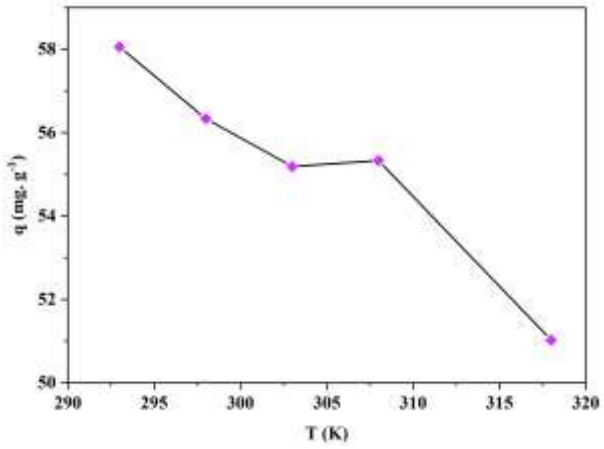

Figure 9: Effect of solution temperature on the adsorption of MC on bridged bentonite (C_0 = 10 mg. L^{-1}, v = 250 rpm, t = 30 min).

The figure shows that a rise in temperature is combined with a discount within the amount of MC dye adsorption from 58 mg. g^{-1} (at 293 K) to 51 mg. g^{-1} (at 318 K). This phenomenon indicates that the reaction is exothermic, and the increase in temperature will reduce the surface activity, which is not conducive to the adsorption mechanism (Degbe et al., 2016). This might flow from to the decrease of the adsorption force between the dye species and therefore the surface-active sites of the adsorbent due to the increase in temperature (Boumchita et al.).

Influence of contact time on adsorption and kinetic models

The kinetic study of the adsorption is essential for the determination of the time necessary to reach the equilibrium of

adsorption i.e., a state of saturation of adsorbent by the adsorbate. It also allows to determine, in a comparative way, the quantity of adsorbed dye according to the contact time.

We followed the adsorption kinetics of MC for a mass equivalent to 0.015 g. Figure 10 (a) illustrate the evolution of the amount of adsorbed dye according to the stirring time. It shows that there is a strong increase in adsorption for the first minutes of contact about 41.05 mg. g^{-1} after 5 minutes; an equilibrium state is noticed after 15 minutes of stirring with an adsorbed amount equal to 59.30 mg. g^{-1} and it remained almost unchanged until the end of the experiment.

We can consider from the results obtained that there are two stages of methylthionine chloride fixation on the bentonite. A first rapid part which may be explained by the abundant availability of active sites on the surface of the bentonite, then it becomes slow until the stabilization after 15 minutes which corresponds to the equilibrium following the occupation of all the sites and consequently the saturation of the adsorbent and the disappearance of the dye from the solution.

Kinetic modelling

Several kinetic models can be used to model the mechanism of adsorption of a fixed body on an adsorbent. We have adopted three kinetic models namely the pseudo first order PPO (b), the pseudo second order PSO (c) and the intra-particle diffusion DIP (d).

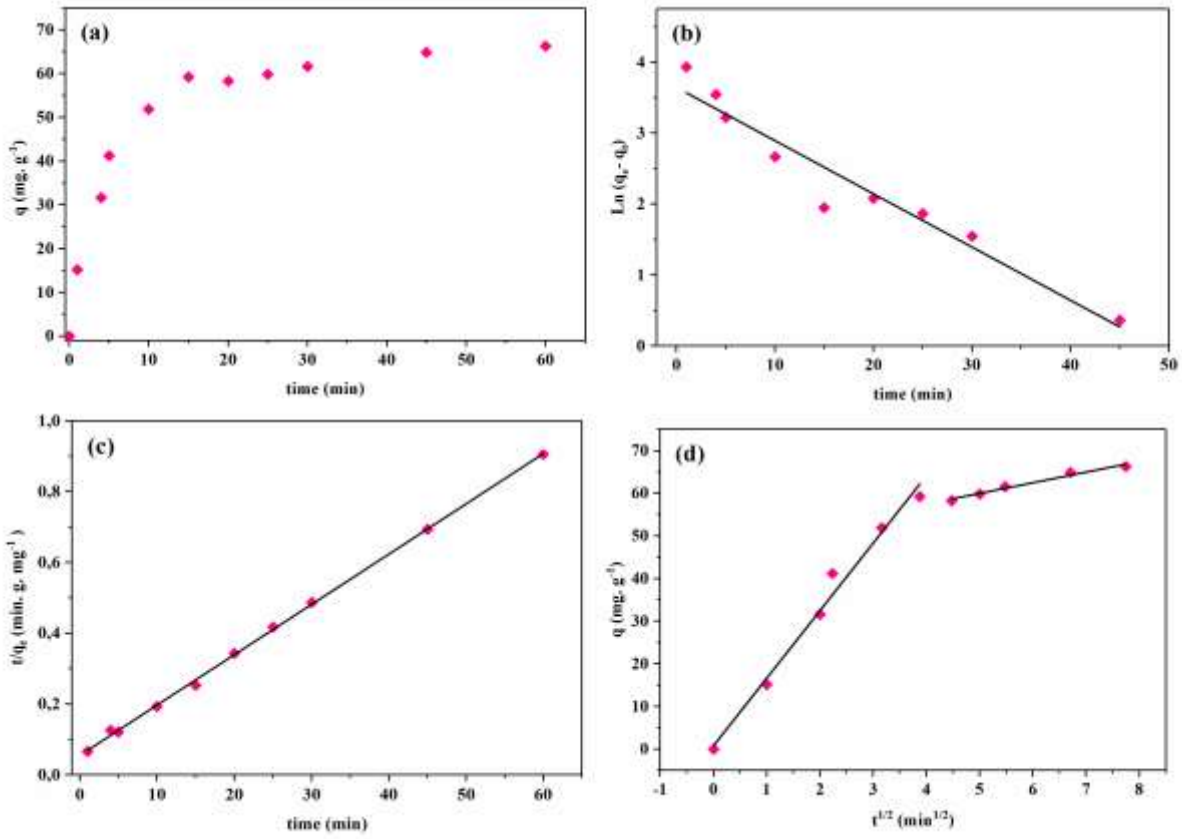

Figure 10: Effect of contact time on the adsorption of MC on bridged bentonite (a). Kinetic models of Pseudo first order (b), pseudo second order (c), intra-particle diffusion (d).

From the previously plotted graphs, we have grouped the different constants of each model namely the velocity constants, the correlation coefficients and the quantity adsorbed at equilibrium in Table 2.

According to the findings obtained shown in (Table 2), it is important to notice the theoretically determined value of the maximum adsorption capacity at equilibrium for the pseudo first order is completely different from the one measured experimentally, on the other hand, the pseudo second order model is more adequate to model the kinetics of adsorption of methylthionine chloride by bridged bentonite with a significant correlation coefficient of the order of 0.936, thus, the value of the equilibrium adsorbed amount calculated by this model coincides with that determined experimentally.

Generally, for the intra-particle diffusion model to be applicable, the curve must be linear. However, in some cases the curve of this model can take a multilinear form justifying that the adsorption process is controlled by several steps (Budnyak et al., 2020; Dawood & Sen, 2012).

Table 2: Values of the correlation coefficients of the different kinetic models.

Kinetic models	$q_{e\ exp}$ **(mg. g^{-1})**	**66,288**
Pseudo first order	k_1 (min^{-1})	0,0795
	$q_{e,\ calc}$ (mg. g^{-1})	43,306
	R^2	**0,936**
Pseudo second order	K_2 (min^{-1})	3,65. 10^{-4}
	$q_{e,\ calc}$ (mg. g^{-1})	70,422
	R^2	**0,999**
intra-particle diffusion	K_{id1} (mg. g^{-1}.min$^{1/2}$)	15,84
	C_1 (mg. g^{-1})	0,80
	R_1^2	**0,985**
	K_{id2} (mg. g^{-1}.min$^{1/2}$)	2,49
	C_2 (mg. g^{-1})	47,52
	R_2^2	**0,977**

For MC adsorption, the presence of two sections is clearly observed, indicating that the adsorption mechanism during this case is controlled by two steps: The first is related to mass transfer to the outer surface of the bentonite followed by intra-particle diffusion. The diffusion constant kid decreases remarkably with time, which may be attributed to the facts that in the initial state the large diffusion of the dye inside the structure of the adsorbent causes a significant reduction of the pore number available for diffusion which reduces the movement of molecules in these pores and subsequently the diffusion of solute (Dotto & Pinto, 2011).

Adsorption isotherms and modelling of adsorption isotherms

By studying the adsorption isotherms, the adsorption capacity of the MC adsorbate on the bentonite and the type of adsorption mechanism can be determined for this, our research is carried out by changing the initial concentration for a mass of 0.015 g, at the solution's pH and at an ambient temperature. Figure 11, illustrates the variation of the equilibrium adsorbed amount depends of the equilibrium concentration.

The figure 11 (a) demonstrates that the adsorption isotherm of MC on bentonite corresponds to the type L isotherm (called Langmuir) according to the classification of Giles & *al*. (Gil et al., 2011), This type means that the quantity of adsorption increases because the concentration of the adsorbate increases. Moreover, this isotherm indicates a strong affinity between the surface of the adsorbent and therefore the reactive molecules of the dye (Giles et al., 1974).

Modelling of adsorption isotherms

The objective is to establish the models that can accurately describe the

experimental results of the sorption isotherm of MC by B-Acr and to specify the parameters obtained that provide information about the adsorption mechanism, surface properties and adsorbent-adsorbate affinities. For this purpose, the three most commonly used models are used, which include the Langmuir (b), Freundlich (c) and Temkin (d) models.

From the results obtained, we summarized the different Langmuir, Freundlich and Temkin model constants in the table 3.

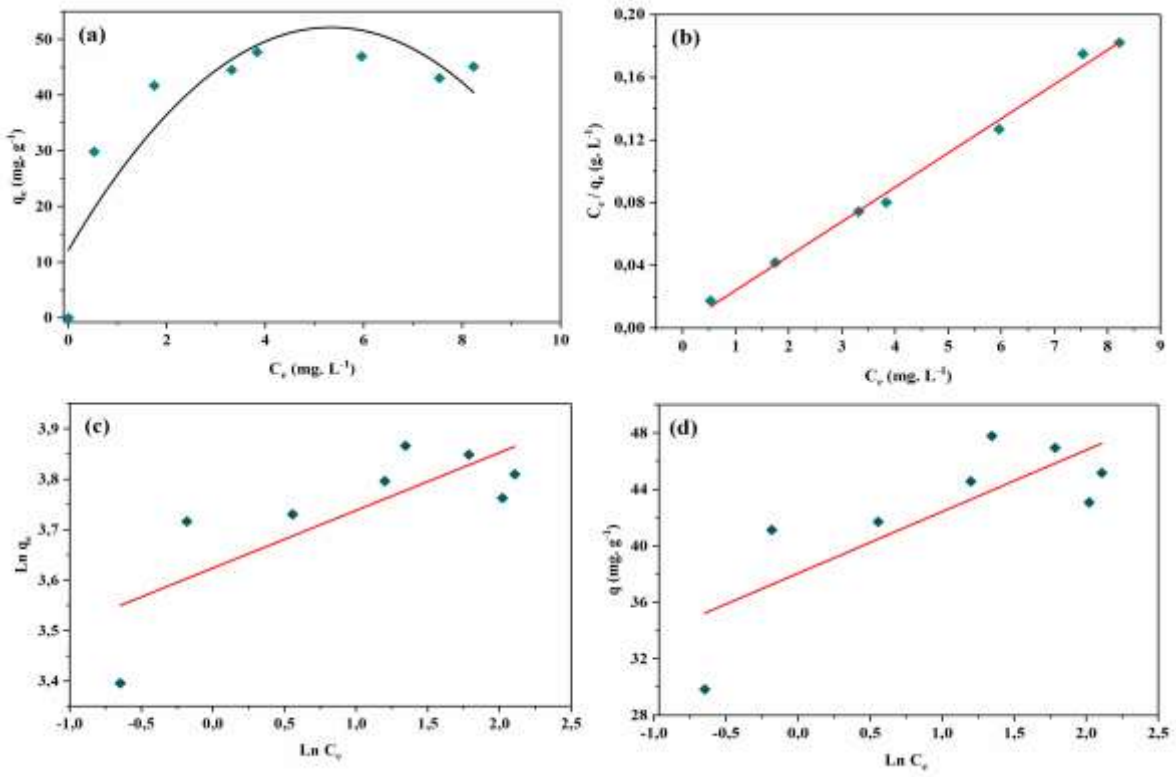

Figure 11: Adsorption isotherm of MC on bridged bentonite (a). Langmuir (b), Freundlich (c) and Temkin (d) equation modelling of the adsorption isotherm of MC on bridged bentonite.

Table 3: Different parameters of Langmuir, Freundlich and Temkin constants and corr-elation coefficient.

Langmuir	
q_m (mg. g^{-1})	45,682
K_L (L. mg^{-1})	9,28
R_L	0,011
R^2	**0,994**
Freundlich	
1/n	0,114
N	8,745
K_F	0,027
R^2	**0,617**
Temkin	
B	0,027
a_T (L. mg^{-1})	78,371
b_T (Kj. mol^{-1})	107,34
R^2	0,379

It is of particular interest to observe that our substrate has a cationic structure and

therefore it adsorbs more easily (Xie et al., 2021). This fact is confirmed on the one hand, by the value of the maximum retention capacity of this dye which is about 45.682 mg. g^{-1} and an excellent correlation coefficient (R^2 = 0.994), and on the other hand, by the dimensionless parameter R_L < 1 which confirms the favourability of the Langmuir isotherm (R_L=0.011) (Akpor et al., 2018).

From the results obtained from Graph 11 (c) and Table 3, the adsorption of methylthionine chloride by bridged bentonite appears unfavourable according to the Freundlich model. (R^2 = 0.617). K_F is a sign of the adsorption capacity, i.e., the larger the K_F value, the more significant the adsorption, which is not the case for this study (K_F = 0.027) (Vimonses et al., 2009). The other Freundlich constant, (n = 8.745), If n is less than 1, it means that adsorption may be a chemical process; while n greater than 1 is related to adsorption and physical processes (Mohammad et al., 2010; Salleh et al., 2011). Therefore, it can be concluded that the retention of MC by bentonite is physisorption (Sen et al., 2011).

From the results obtained previously, we find that the Temkin model is not adequate to linearize the adsorption of MC this is confirmed by a correlation coefficient R^2 = 0.379.

Thus, the adsorption energy constant (b_T = 107.34 Kj. mol^{-1}) is positive indicating that the adsorption process is exothermic.

Thermodynamic study

In the interests to apprehend the thermodynamic phenomenon of the adsorption of the dye MC by the bentonite, we followed the decolouration by varying the temperature of the dyed solutions from 293 K to 318 K.

The evolution of Ln K_d as a function of 1/T (Figure 12), allowed us to deduce the thermodynamic quantities relating to the studied adsorbate/adsorbent system which are gathered in the next table.

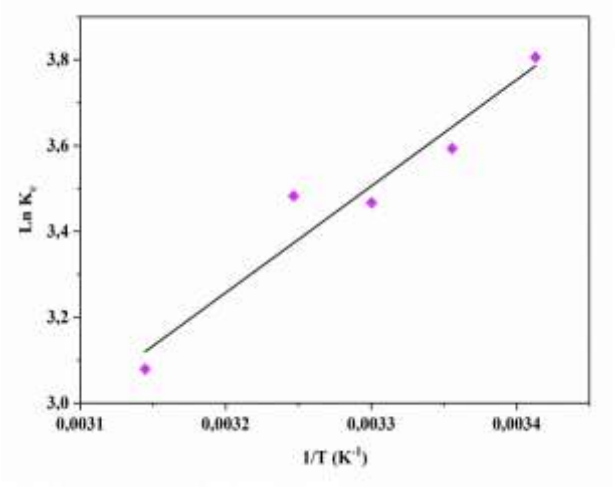

Figure 12: Effect of temperature on the distribution constant of the phenomenon of adsorption of MC on B-Acr.

From Figure 12 the data in Table 4, we see that the free enthalpy values are negative (ΔG°<0) and increase with increasing temperature which indicates that the process of removal of methylthionine chloride by bentonite is spontaneous.

Table 4: Thermodynamic parameters of MC adsorption on bridged bentonite.

T(K)	ΔH°(kJ. mol^{-1})	ΔS°(J.K^{-1}. mol^{-1})	R^2	ΔG°(kJ. mol^{-1})
293	-20,617	-38,984	0,939	-9,195
298				-8,999
303				-8,805
308				-8,610
318				-8,220

The calculated value of enthalpy is also negative (ΔH°< 0), which shows that this

process is exothermic confirming the results obtained previously, also, ΔH° is positive shows that it is a physisorption (4.93 Kcal. mol^{-1}). On the other hand, the negative value of the standard entropy ΔS° are often wont to describe the randomness at the MC-bentonite interface and suggests that the adsorption occurs with increasing order at the solid-solution interface (Elmoubarki et al., 2015; Kumar et al., 2010).

It seemed interesting to us to compare the results we obtained in this study with those obtained for a raw bentonite where we noticed the big difference

We can see that methylthionine chloride adsorbs much faster and the quantities adsorbed at equilibrium are much higher in the case of B-Acr than for raw bentonite (Batana et al., 2019).

4. Conclusion

The experimental techniques used allowed us to characterize the bentonite studied and to highlight its composition. We have thus established that this bentonite is essentially composed of Kaolinite, Illite and Montmorillonite as associated clay minerals. These results have also highlighted the richness of this bentonite in Quartz which results in a high proportion of Silica. Maghnia bentonite, like other bentonites, is suitable to be used within the dye treatment method of wastewater dye treatment. The removal of MC is influenced by the solution's pH, the contact time, the mass of the adsorbent and the temperature. The maximum removal capacity of MC (45.682 mg. g^{-1}) was reached at 15 minutes. The adsorption capacity of MC increased with increasing pH from 6 to 10 as a result of the strong affinity among the surface of negatively charged bridged bentonite with positively charged MC and decreased with temperature (adsorption process is exothermic) and with adsorbent mass which explains the non-saturation of adsorption sites.

The kinetic modelling of MC adsorption on bridged bentonite followed the pseudo-second order model and intra-particle diffusion is not the only limiting step. The adsorption isotherm is linearized according to the Langmuir model with a correlation coefficient R^2 greater than 0.994 and maximum adsorbed amount equal to 45.682 mg. g^{-1}. The values of the thermodynamic parameters are negative (ΔH°, ΔG°, and $\Delta S^{\circ} < 0$) indicating that the process of methylthionine chloride removal by bentonite is exothermic, spontaneous, and with order increase at the solid-solution interface.

Prospects

These preliminary studies suggest that bentonite can be effectively used for the adsorption of MC and other dyes from industrial wastewater which is a priority as well as studying the regeneration of the adsorbent in the case improve the economic feasibility

Declaration of competing interest

The authors declare no conflict of interest.

Data Availability Statement

Data will be made available upon reasonable request.

5. References

Ahmad, A., Mohd-Setapar, S. H., Chuong, C. S., Khatoon, A., Wani, W. A., Kumar, R., & Rafatullah, M. (2015). Recent advances in new generation dye removal technologies: novel search for approaches to reprocess wastewater. *RSC advances*, *5*(39), 30801-30818.

Ahmed, H. R., Raheem, S. J., & Aziz, B. K. (2017). Removal of Leishman stain from aqueous solutions using natural

clay of Qulapalk area of Kurdistan region of Iraq. *Karbala International Journal of Modern Science*, *3*(3), 165-175.

Akpor, O., Deborah, J. E., & Oluba, O. M. (2018). Comparative decolouration of crystal violet dye using ChickenFeather fibre, chemical oxidation and bacterial cells. *Journal of Environmental Science and Technology*, *11*(5), 246-253.

Annadurai, G., Juang, R.-S., & Lee, D.-J. (2002). Use of cellulose-based wastes for adsorption of dyes from aqueous solutions. *Journal of hazardous materials*, *92*(3), 263-274.

Arenas, C. N., Vasco, A., Betancur, M., & Martínez, J. D. (2017). Removal of indigo carmine (IC) from aqueous solution by adsorption through abrasive spherical materials made of rice husk ash (RHA). *Process Safety and Environmental Protection*, *106*, 224-238.

Azbar, N., Yonar, T., & Kestioglu, K. (2004). Comparison of various advanced oxidation processes and chemical treatment methods for COD and color removal from a polyester and acetate fiber dyeing effluent. *Chemosphere*, *55*(1), 35-43.

Azizian, S., Haerifar, M., & Bashiri, H. (2009). Adsorption of methyl violet onto granular activated carbon: Equilibrium, kinetics and modeling. *Chemical Engineering Journal*, *146*(1), 36-41.

Batana, F., Taouti, M., & Guibadj, A. (2019). Cinétique de l'adsorption du bleu de méthylène sur bentonite brute et traitée. *Algerian Journal of Environmental Science and Technology*, *5*(4).

Benfarhi, S., Decker, C., Keller, L., Zahouily, K., & Bendaikha, T. (2005). Synthèse de matériaux hybrides polymère-argile par polymérisation photo-induite. Journal de Physique IV (Proceedings),

Bessaha, F., Mahrez, N., Marouf-Khelifa, K., Çoruh, A., & Khelifa, A. (2019). Removal of Congo red by thermally and chemically modified halloysite: equilibrium, FTIR spectroscopy, and mechanism studies. *International Journal of Environmental Science and Technology*, *16*(8), 4253-4260.

Boumchita, S., Lahrichi, A., Benjelloun, Y., Lairini, S., Nenov, V., & Zerrouq, F. Elimination d'un colorant cationique dans une solution aqueuse par un déchet alimentaire: Epluchure de pomme de terre [Removal of cationic dye from aqueous solution by a food waste: Potato peel].

Budnyak, T. M., Błachnio, M., Slabon, A., Jaworski, A., Tertykh, V. A., Deryło-Marczewska, A., & Marczewski, A. W. (2020). Chitosan deposited onto fumed silica surface as sustainable hybrid biosorbent for Acid Orange 8 dye capture: Effect of temperature in adsorption equilibrium and kinetics. *The Journal of Physical Chemistry C*, *124*(28), 15312-15323.

Chebbi, R., Fadel, A., & Aidi, A. (2021). The Elimination by Natural Algerian Clay of Chromium Ions from Salt Water. Annales de Chimie-Science des Matériaux,

Dawood, S., & Sen, T. K. (2012). Removal of anionic dye Congo red from aqueous solution by raw pine and acid-treated pine cone powder as adsorbent: equilibrium, thermodynamic, kinetics, mechanism and process design. *Water research*, *46*(6), 1933-1946.

Degbe, A., Koriko, M., Tchegueni, S., Aziable, E., Tchakala, I., Hafidi, M., El Meray, M., & Tchangbedji, G. (2016). Biosorption of methylene blue solution: Comparative study of the cactus (Opuntia ficusindica) of Lmé (CL) and Marrakech (CM). *J Mater Environ Sci*, *7*, 4786-4794.

Dotto, G., & Pinto, L. (2011). Adsorption of food dyes acid blue 9 and food yellow 3 onto chitosan: Stirring rate effect in kinetics and mechanism. *Journal of hazardous materials*, *187*(1-3), 164-170.

Elmoubarki, R., Mahjoubi, F., Tounsadi, H., Moustadraf, J., Abdennouri, M., Zouhri, A., El Albani, A., & Barka, N.

(2015). Adsorption of textile dyes on raw and decanted Moroccan clays: kinetics, equilibrium and thermodynamics. *Water resources and industry*, *9*, 16-29.

Elwakeel, K. Z., Elgarahy, A. M., Al-Bogami, A. S., Hamza, M. F., & Guibal, E. (2021). 2-Mercaptobenzimidazole-functionalized chitosan for enhanced removal of methylene blue: Batch and column studies. *Journal of Environmental Chemical Engineering*, *9*(4), 105609.

Er-ramly, A., & Ider, A. (2014). Physico-chemical and mineralogical characterization of a Moroccan bentonite (Azzouzet) and determination of its nature and its chemical structure. *International Journal of Materials Science and Applications*, *3*, 42-48.

Ghosh, S. K., Mandal, M., Kundu, S., Nath, S., & Pal, T. (2004). Bimetallic Pt–Ni nanoparticles can catalyze reduction of aromatic nitro compounds by sodium borohydride in aqueous solution. *Applied Catalysis A: General*, *268*(1-2), 61-66.

Gil, A., Assis, F., Albeniz, S., & Korili, S. (2011). Removal of dyes from wastewaters by adsorption on pillared clays. *Chemical Engineering Journal*, *168*(3), 1032-1040.

Giles, C. H., Smith, D., & Huitson, A. (1974). A general treatment and classification of the solute adsorption isotherm. I. Theoretical. *Journal of colloid and interface science*, *47*(3), 755-765.

Hameed, B. (2007). Equilibrium and kinetics studies of 2, 4, 6-trichlorophenol adsorption onto activated clay. *Colloids and Surfaces A: Physicochemical and Engineering Aspects*, *307*(1-3), 45-52.

Kannan, N., & Sundaram, M. M. (2001). Kinetics and mechanism of removal of methylene blue by adsorption on various carbons—a comparative study. *Dyes and pigments*, *51*(1), 25-40.

Kara, M., Yuzer, H., Sabah, E., & Celik, M. (2003). Adsorption of cobalt from aqueous solutions onto sepiolite. *Water research*, *37*(1), 224-232.

Karim, A., Mounir, B., Hachkar, M., Bakasse, M., & Yaacoubi, A. (2010). Élimination du colorant basique «Bleu de Méthylène» en solution aqueuse par l'argile de Safi. *Revue des sciences de l'eau/Journal of Water Science*, *23*(4), 375-388.

Kaur, S., Rani, S., & Mahajan, R. K. (2013). Adsorption kinetics for the removal of hazardous dye congo red by biowaste materials as adsorbents. *Journal of Chemistry*, *2013*.

Kumar, P. S., Ramalingam, S., Senthamarai, C., Niranjanaa, M., Vijayalakshmi, P., & Sivanesan, S. (2010). Adsorption of dye from aqueous solution by cashew nut shell: studies on equilibrium isotherm, kinetics and thermodynamics of interactions. *Desalination*, *261*(1-2), 52-60.

Lv, L., He, J., Wei, M., Evans, D., & Zhou, Z. (2007). Treatment of high fluoride concentration water by MgAl-CO3 layered double hydroxides: Kinetic and equilibrium studies. *Water research*, *41*(7), 1534-1542.

Makar, J. M., & Chan, G. W. (2008). End of the induction period in ordinary Portland cement as examined by high-resolution scanning electron microscopy. *Journal of the American ceramic society*, *91*(4), 1292-1299.

Marsal, A., Bautista, E., Ribosa, I., Pons, R., & Garcia, M. (2009). Adsorption of polyphenols in wastewater by organo-bentonites. *Applied Clay Science*, *44*(1-2), 151-155.

Mohammad, M., Maitra, S., Ahmad, N., Bustam, A., Sen, T., & Dutta, B. K. (2010). Metal ion removal from aqueous solution using physic seed hull. *Journal of hazardous materials*, *179*(1-3), 363-372.

Nabbou, N., Belhachemi, M., Boumelik, M., Merzougui, T., Lahcene, D., Harek, Y., Zorpas, A. A., & Jeguirim, M.

(2019). Removal of fluoride from groundwater using natural clay (kaolinite): Optimization of adsorption conditions. *Comptes Rendus Chimie*, *22*(2-3), 105-112.

Naranjo, P. M., Molina, J., Sham, E. L., & Torres, E. M. F. (2015). Synthesis and characterization of hdtma-organoclays: insights into their structural properties. *Quimica Nova*, *38*, 166-171.

Ordonez, D., Valencia, A., Chang, N.-B., & Wanielista, M. P. (2020). Synergistic effects of aluminum/iron oxides and clay minerals on nutrient removal and recovery in water filtration media. *Journal of Cleaner Production*, *275*, 122728.

Panneerselvam, P., Morad, N., & Tan, K. A. (2011). Magnetic nanoparticle (Fe3O4) impregnated onto tea waste for the removal of nickel (II) from aqueous solution. *Journal of hazardous materials*, *186*(1), 160-168.

Patil, A., & Shrivastava., V. (2010). Alternanthera bettzichiana plant powder as low cost adsorbent for removal of Congo red from aqueous solution. *International Journal of ChemTech Research*, *2*(2), 842–850.

Pérez-Marín, A., Zapata, V. M., Ortuno, J., Aguilar, M., Sáez, J., & Lloréns, M. (2007). Removal of cadmium from aqueous solutions by adsorption onto orange waste. *Journal of hazardous materials*, *139*(1), 122-131.

Praus, P., Turicová, M., Študentová, S., & Ritz, M. (2006). Study of cetyltrimethylammonium and cetylpyridinium adsorption on montmorillonite. *Journal of colloid and interface science*, *304*(1), 29-36.

Sakr, F., Sennaoui, A., Elouardi, M., Tamimi, M., & Assabbane, A. (2015). Étude de l'adsorption du Bleu de Méthylène sur un biomatériau à base de Cactus (Adsorption study of Methylene Blue on biomaterial using cactus). *Journal of materials and Environmental Science*, *6*(2), 397-406.

Salleh, M. A. M., Mahmoud, D. K., Karim, W. A. W. A., & Idris, A. (2011). Cationic and anionic dye adsorption by agricultural solid wastes: a comprehensive review. *Desalination*, *280*(1-3), 1-13.

Sarier, N., Onder, E., & Ersoy, S. (2010). The modification of Na-montmorillonite by salts of fatty acids: An easy intercalation process. *Colloids and Surfaces A: Physicochemical and Engineering Aspects*, *371*(1-3), 40-49.

Sen, T. K., Afroze, S., & Ang, H. (2011). Equilibrium, kinetics and mechanism of removal of methylene blue from aqueous solution by adsorption onto pine cone biomass of Pinus radiata. *Water, Air, & Soil Pollution*, *218*(1), 499-515.

Tahir, N., Bhatti, H. N., Iqbal, M., & Noreen, S. (2017). Biopolymers composites with peanut hull waste biomass and application for Crystal Violet adsorption. *International Journal of Biological Macromolecules*, *94*, 210-220.

Ting, A. S. Y., Cheng, C. K. W., & Santiago, K. A. A. (2021). Decolourization of malachite green dye by endolichenic fungi from the lichen Usnea sp.: A novel study on their dye removal potential. *Journal of King Saud University-Science*, *33*(7), 101579.

Vakili, M., Rafatullah, M., Salamatinia, B., Abdullah, A. Z., Ibrahim, M. H., Tan, K. B., Gholami, Z., & Amouzgar, P. (2014). Application of chitosan and its derivatives as adsorbents for dye removal from water and wastewater: A review. *Carbohydrate polymers*, *113*, 115-130.

Vicente-Rodríguez, M. A., Suarez, M., Bañares-Muñoz, M. A., & de Dios Lopez-Gonzalez, J. (1996). Comparative FT-IR study of the removal of octahedral cations and structural modifications during acid treatment of several silicates. *Spectrochimica Acta Part A: Molecular and Biomolecular Spectroscopy*, *52*(13), 1685-1694.

Vimonses, V., Lei, S., Jin, B., Chow, C. W., & Saint, C. (2009). Kinetic study and equilibrium isotherm analysis of Congo Red adsorption by clay

materials. *Chemical Engineering Journal*, *148*(2-3), 354-364.

Xie, J., Yamaguchi, T., & Oh, J.-M. (2021). Synthesis of a mesoporous Mg–Al–mixed metal oxide with P123 template for effective removal of Congo red via aggregation-driven adsorption. *Journal of Solid State Chemistry*, *293*, 121758.

Yang, S., Guo, M., Yang, E., & Zhang, H. (2018). Study on preparation and performance of high swelling bentonite. *Matéria (Rio de Janeiro)*, *23*.

Yu, B., Zhang, Y., Shukla, A., Shukla, S. S., & Dorris, K. L. (2000). The removal of heavy metal from aqueous solutions by sawdust adsorption—removal of copper. *Journal of hazardous materials*, *80*(1-3), 33-42.

Yuan, P., Tan, D., Aannabi-Bergaya, F., Yan, W., Fan, M., Liu, D., & He, H. (2012). Changes in structure, morphology, porosity, and surface activity of mesoporous halloysite nanotubes under heating. *Clays and Clay Minerals*, *60*(6), 561-573.